

# Axions on a Hyperbolic Ride: Geometric Suppression of CMB Isocurvature and a Blue-Tilted Spectrum

Sai Chaitanya Tadepalli\*

Physics Department, Indiana University, Bloomington, IN 47405, USA

(Dated: February 2, 2026)

CMB limits on cold-dark-matter isocurvature are often interpreted as excluding the simultaneous realization of high-scale inflation and large QCD axion decay constants in pre-inflationary Peccei–Quinn (PQ) scenarios. We show that this conclusion can be evaded by exploiting *field-space geometry*. For a minimal complex PQ scalar with a  $U(1)$ -symmetric potential and nonlinear sigma-model kinetic term  $d\sigma^2 = dR^2 + f^2(R)d\theta^2$ , a curved target-space metric endows the axion fluctuation with a time-dependent geometric mass during inflation, suppressing isocurvature without explicit PQ breaking and without extreme radial displacements. Specializing to a hyperbolic metric  $f(R) = L \sinh(R/L)$  with curvature scale  $L$ , we find that for  $R \gtrsim L$  the canonically normalized angular mode can be generically  $\mathcal{O}(H_{\text{inf}})$ -heavy during radial slow-roll, dynamically damping CMB-scale fluctuations while producing a characteristic blue-tilted isocurvature spectrum. As a result, inflationary Hubble scales as large as  $H_{\text{inf}} \sim 10^{13}$  GeV can be compatible with  $f_a \sim 10^{14}\text{--}10^{16}$  GeV, reopening parameter space usually regarded as excluded. We present numerical benchmarks and a semi-analytic template that relates the scale-dependence of isocurvature to the geometric lever arm  $R/L$ , providing a direct phenomenological probe on PQ field-space geometry.

## I. INTRODUCTION

The QCD axion provides a dynamical solution to the strong-CP problem and is a well-motivated dark matter (DM) candidate [1–10]. In the pre-inflationary PQ-breaking scenario, inflation homogenizes the axion field over our observable patch, leaving a coherent background misalignment angle  $\theta_i$ . However, quantum fluctuations generated during inflation persist as cold-dark-matter isocurvature perturbations, while the axion density also carries the usual adiabatic mode inherited from the primordial curvature perturbation. Current CMB limits on the isocurvature fraction in [11–13] therefore translate into a stringent constraint on high-scale inflation as a function of  $(f_a, \theta_i)$ , sharply disfavoring a vast regime of large axion decay constant  $f_a$  (e.g. near the GUT scale) together with  $H_{\text{inf}} \sim 10^{13}$  GeV [14].

The axion isocurvature bound has motivated three main classes of proposals. (i) *Heavy axion during inflation*: suppress fluctuations by making the angular mode heavy,  $m_a \gtrsim H_{\text{inf}}$ , so that superhorizon perturbations are exponentially damped. This can come from a temporarily modified axion potential (enhanced QCD during inflation [15–18], curvature/higher-dimensional terms [19], monodromy/BF-type masses [20]) or SUSY/multi-field transitions that leave a light QCD axion only later [21]. Such mechanisms often require explicit PQ-breaking during inflation and satisfying axion-quality/strong-CP alignment at late times [22, 23]. (ii) *Large effective decay constant*: suppress fluctuations by displacing the radial field ( $R$ ) so that  $R \gg f_a$ , and hence the spectrum is suppressed by  $(H_{\text{inf}}/(R\theta_i))^2$  [21, 24–32]. In the minimal quartic PQ model this tends to force tiny

quartic coefficient  $\lambda$ , large excursions (EFT sensitivity), and complicated post-inflationary dynamics (resonance/fragmentation), with the highest- $H_{\text{inf}}$  regime especially delicate [33]. (iii) *Blue-tilted isocurvature*: use out-of-equilibrium PQ dynamics so the rolling (or rotating) radial background induces a time-dependent mass for angular fluctuations, suppressing CMB modes while enhancing smaller scales [34, 35]. Achieving large blue-tilted spectra over a long range of scales are easiest with effectively quadratic radial evolution (e.g. Hubble masses). However, pure quartic potential typically yield only a short range unless additional dynamics (e.g. sustained rotation) is present [36].

In this work we present a minimal,  $U(1)$  conserving alternative based on field-space geometry. Curved internal field-space metrics are well known to generate effective masses and characteristic scale-dependence for entropic/isocurvature modes in covariant sigma-model systems [37–41]. In this *Letter* we apply this mechanism directly to the PQ field and show that a hyperbolic field-space metric generically endows the angular fluctuation with a geometric, time-dependent effective mass during inflation, without explicit PQ breaking in the axion potential. This dynamically suppresses CMB-scale axion isocurvature, while the evolving mass produces a distinctive blue-tilted isocurvature spectrum on smaller scales. As a result, viable parameter space with  $H_{\text{inf}} \sim 10^{13}$  GeV and large  $f_a$  (e.g.  $\lesssim 10^{16}$  GeV) can be reopened without requiring the extreme displacements  $R_{\text{inf}}/f_a \sim 10^4\text{--}10^5$  or tiny quartic coefficients  $\lesssim \mathcal{O}(10^{-16})$ . We further provide a compact phenomenological template relating the isocurvature spectral index to the field-space curvature scale, thereby promoting measurements of isocurvature scale-dependence to a direct probe of PQ field-space geometry and enabling targeted searches in future analyses.

The paper is organized as follows. Section II reviews the axion isocurvature constraint, Sec. III introduces

\* saictade@iu.edu

the hyperbolic PQ field-space framework, and Sec. IV presents benchmarks and resulting spectra. We conclude in Sec. V. Appendices A, B and C give a UV-motivated origin for the hyperbolic metric, a semi-analytic data-facing template, and relevant derivations respectively.

## II. THE STANDARD QCD AXION ISOCURVATURE PROBLEM

In the pre-inflationary PQ scenario, if the axion field ( $a(x) = f_{\text{eff}}\theta(x)$ ) is light during inflation, its superhorizon fluctuations are set by the de Sitter result

$$\delta a \simeq \frac{H_{\text{inf}}}{2\pi}, \quad \delta\theta \simeq \frac{\delta a}{f_{\text{eff}}(t_*)}, \quad (1)$$

where  $f_{\text{eff}}(t_*)$  is the effective decay constant at CMB horizon exit (typically  $f_{\text{eff}} = f_a$  in minimal models), and  $\theta_i$  is the misalignment angle. See [5] for a review of the discussion in this section.

In the harmonic regime  $|\theta_i| \lesssim 1$ , the axion density scales as  $\rho_a \propto \theta_i^2$ , so the isocurvature mode is

$$\mathcal{S}_a \simeq \frac{\delta\rho_a}{\rho_a} \simeq 2 \frac{\delta\theta}{\theta_i}. \quad (2)$$

If axions constitute a fraction  $r_a \equiv \Omega_a/\Omega_{\text{DM}}$  of the total DM, then the matter isocurvature power is

$$\Delta_{\mathcal{S}}^2(k) \simeq 4r_a^2 \frac{\Delta_\theta^2(k)}{\theta_i^2} \simeq 4r_a^2 \frac{H_{\text{inf}}^2}{(2\pi)^2 f_{\text{eff}}^2(t_*) \theta_i^2}, \quad (3)$$

which is approximately scale invariant in the light-axion limit. CMB data constrain the isocurvature fraction at the percent level near the pivot  $k_* = 0.002 \text{ Mpc}^{-1}$ , implying (for  $r_a \simeq 1$  and  $f_{\text{eff}} = f_a$ )

$$\frac{H_{\text{inf}}}{f_a \theta_i} < 2.8 \times 10^{-5}. \quad (4)$$

For QCD axions making all of DM via misalignment in a standard thermal history,  $\theta_i$  is fixed by  $f_a$  through the relic abundance. Using the usual scaling  $\Omega_a \propto f_a^{7/6} \theta_i^2$  (up to  $\mathcal{O}(1)$  uncertainties),  $\Omega_a = \Omega_{\text{DM}}$  gives ([6, 42])

$$\theta_i \equiv \theta_{i,\text{QCD}} \simeq \left( \frac{7.4 \times 10^{11} \text{ GeV}}{f_a} \right)^{7/12}. \quad (5)$$

This relation assumes the PQ radial field has relaxed to its late-time vacuum well before the QCD epoch, so the decay constant at the onset of oscillations is  $f_a$ .

Fig. 1 displays the resulting tension in the  $(H_{\text{inf}}, f_a)$  plane. If the inflationary effective decay constant is enhanced to  $f_{\text{eff}} = \kappa f_a$ , the bound is relaxed accordingly; combining Eqs. (4) and (5) yields the schematic scaling

$$\frac{f_a}{2.04 \times 10^{18} \text{ GeV}} > \left( \frac{H_{\text{inf}}}{10^{10} \text{ GeV}} \frac{1}{\kappa} \right)^{12/5}. \quad (6)$$

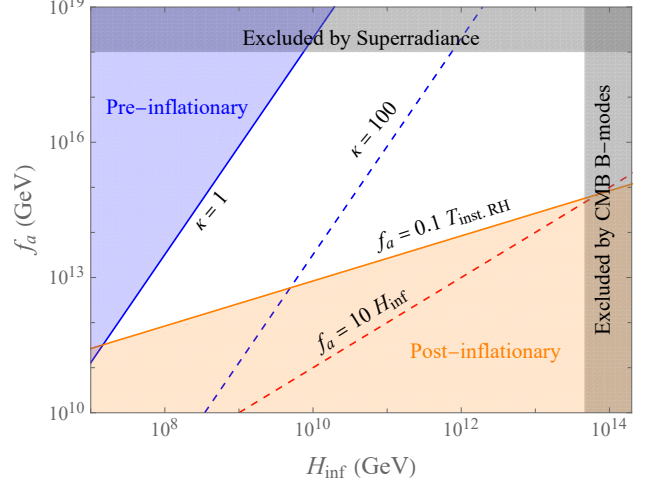


FIG. 1. Illustrative constraints in the  $(H_{\text{inf}}, f_a)$  plane for pre-inflationary QCD axion DM from misalignment. For the standard flat-metric case  $f_{\text{eff}} = f_a$ , the isocurvature bound restricts QCD axion to the blue shaded region. Gray bands indicate additional excluded regions. *In this work, we show that the white region can be reopened using geometric suppression.* (Redrawn with inspiration from [33].)

$T_{\text{inst.RH}}$  is the instantaneous reheating temperature and the orange solid line marks the upper boundary of the region for PQ restoration post-inflation. In flat-metric quartic PQ models, realizing simultaneously  $H_{\text{inf}} \simeq 10^{13} \text{ GeV}$  and  $f_a \sim 10^{16} \text{ GeV}$  typically forces  $\kappa \gtrsim 10^4$ , often into a regime where the spectator/EFT description is difficult to control. This motivates alternative suppression mechanisms.

## III. HYPERBOLIC PQ FIELD-SPACE AND GEOMETRIC SUPPRESSION

During inflation we take a quasi-de Sitter background with spatially flat FRW metric

$$ds^2 = -dt^2 + a(t)^2 dx^2, \quad a(t) \simeq e^{Ht}, \quad (7)$$

where  $H \simeq H_{\text{inf}}$  is approximately constant. We consider a spectator PQ complex scalar  $\Phi$  with a  $U(1)$ -symmetric potential and allow a nontrivial internal field-space metric. Writing

$$\Phi(x) = \frac{R(x)}{\sqrt{2}} e^{i\theta(x)}, \quad (8)$$

we adopt the diagonal sigma-model form

$$d\sigma^2 = dR^2 + f^2(R) d\theta^2, \quad (9)$$

so that the action can be written as

$$S = \int d^4x \sqrt{-g} \left[ -\frac{1}{2} (\partial R)^2 - \frac{1}{2} f^2(R) (\partial\theta)^2 - V(R) \right], \quad (10)$$

with  $f^2(R) > 0$  and no explicit  $\theta$ -dependence in  $V$ .

Details and derivations in this section are deferred to the App. C. We work in the vanishing-charge background  $\dot{\theta}_0 = 0$ , for which the homogeneous evolution is purely radial,

$$\ddot{R}_0 + 3H\dot{R}_0 + V_{,R}(R_0) = 0, \quad (11)$$

and is independent of  $f(R)$ . The effect of the curved metric appears in the fluctuations. The radial perturbation obeys

$$\ddot{\delta R} + 3H\dot{\delta R} - \frac{\nabla^2}{a^2}\delta R + V_{,RR}(R_0)\delta R = 0. \quad (12)$$

Defining the canonically normalized angular fluctuation

$$\delta\psi \equiv f(R_0)\delta\theta, \quad (13)$$

one finds

$$\ddot{\delta\psi} + 3H\dot{\delta\psi} - \frac{\nabla^2}{a^2}\delta\psi + m_\psi^2(t)\delta\psi = 0, \quad (14)$$

with the time-dependent effective mass

$$m_\psi^2(t) = \frac{f'}{f}V_{,R}(R_0) - \frac{f''}{f}\dot{R}_0^2, \quad (15)$$

(primes denote derivatives with respect to  $R$ , evaluated on  $R_0(t)$ ). In flat field-space ( $f(R) = R$ ) one recovers  $m_\psi^2 \simeq V_{,R}/R_0$ , so the axial fluctuation has a mass of the same order as the radial mode, and the two evolve with comparable effective masses.

*a. Hyperbolic metric.* We instead consider a constant negative-curvature field-space,

$$d\sigma^2 = dR^2 + L^2 \sinh^2\left(\frac{R}{L}\right) d\theta^2, \quad f(R) = L \sinh\left(\frac{R}{L}\right), \quad (16)$$

with curvature scale  $L > 0$ . See Appendix A for a UV-motivated example that realizes this metric. Then

$$m_\psi^2(t) = \frac{1}{L} \coth\left(\frac{R_0}{L}\right) V_{,R}(R_0) - \frac{1}{L^2} \dot{R}_0^2. \quad (17)$$

For  $R_0 \gtrsim L$  and slow-roll background radial evolution, it is useful to write

$$m_\psi^2(t) \approx H_{\text{inf}}^2 \left( \delta - \frac{\delta^2}{9} \right), \quad (18)$$

where

$$\delta \equiv \xi \frac{m_R^2}{H_{\text{inf}}^2}, \quad \xi \equiv \frac{R_0}{L}, \quad m_R^2 \equiv \frac{V_{,R}(R_0)}{R_0}. \quad (19)$$

The leading geometric contribution is enhanced by the curvature lever arm  $\xi = R_0/L$ , while the subleading negative term encodes the reduction of transverse masses from negative curvature when  $\dot{R}_0 \neq 0$ . In typical slow-roll trajectories the angular mode is initially  $\mathcal{O}(H)$ -heavy (damping CMB-scale fluctuations) and becomes lighter as  $R_0$  relaxes and  $\dot{R}_0$  redshifts. This time dependence generically produces blue-tilted isocurvature: modes exiting earlier (larger scales) are most suppressed, while later-exiting modes (smaller scales) are less suppressed and approach a quasi-plateau once the angular mode becomes effectively light.

	$\lambda$	$f_a/H_{\text{inf}}$	$R_i/H_{\text{inf}}$	$N_{\text{inf}}$	$L/H_{\text{inf}}$
B1	$2 \times 10^{-7}$	$10^1$	$1.5 \times 10^3$	55	$1.1 \times 10^2$
B2	$4 \times 10^{-6}$	$10^1$	$3.5 \times 10^2$	55	$2.1 \times 10^1$
B3	$2 \times 10^{-9}$	$10^3$	$1.5 \times 10^4$	55	$1.1 \times 10^3$

TABLE I. Benchmark parameter choices.

#### IV. BENCHMARK MODELS AND ISOCURVATURE SPECTRUM

We adopt the minimal quartic PQ potential

$$V(R) = \frac{\lambda}{4} (R^2 - f_{\text{PQ}}^2)^2, \quad f_{\text{PQ}} \simeq f_a, \quad (20)$$

with hyperbolic metric Eq. (16) and work in the vanishing charge sector  $\dot{\theta}_0 = 0$ . We evolve the background fields during inflation, using  $N \equiv \ln a$ , and compute fluctuations mode-by-mode with Bunch-Davies initial conditions deep inside the horizon. The angular power spectrum is

$$\Delta_\theta^2(k) \equiv \frac{k^3}{2\pi^2} |\delta\theta_k|^2, \quad \delta\theta_k = \frac{\delta\psi_k}{f(R_0)} \Big|_{\text{late}}. \quad (21)$$

In the harmonic regime, the total matter isocurvature spectrum is

$$\Delta_S^2(k) \simeq \frac{4r_a^2}{\theta_i^2} \Delta_\theta^2(k), \quad (22)$$

evaluated at the end of inflation  $N_{\text{inf}}$ . For QCD axion DM from misalignment, we eliminate  $\theta_i$  using Eq. (5).

We consider three benchmark points B1-B3 (Tab. I), chosen such that the initial curvature lever arm  $\xi_i \equiv R_i/L$  is  $\sim \mathcal{O}(10)$  and CMB-scale isocurvature is suppressed at high  $H_{\text{inf}} \sim 10^{13}$  GeV. The near-degeneracy of B1 and B3 is intentional: in  $H_{\text{inf}}$  units the spectator PQ system has an approximate rescaling symmetry,

$$R \rightarrow \frac{R}{x}, \quad L \rightarrow \frac{L}{x}, \quad f_a \rightarrow \frac{f_a}{x^{24/14}}, \quad \lambda \rightarrow \lambda x^2, \quad (23)$$

which leaves the dimensionless geometry  $(R/L)$  and the radial mass in Hubble units approximately invariant, yielding nearly identical spectra for B1 and B3 despite different  $f_a$ . Benchmark B2 instead illustrates the breadth of viable parameter space at fixed  $f_a/H_{\text{inf}} = 10$  by varying  $(\lambda, R_i/L, L/H_{\text{inf}})$ .

#### A. Results

Fig. 2 shows the mass history for B1. The radial field slow-rolls toward its vacuum, while the hyperbolic metric induces a geometric axial mass. Initially  $m_\psi^2 \sim \mathcal{O}(H_{\text{inf}}^2)$  while  $m_R^2 \ll H_{\text{inf}}^2$ , so modes exiting early are damped. As  $R_0$  decreases and  $\dot{R}_0$  redshifts,  $m_\psi^2/H^2$  falls and the

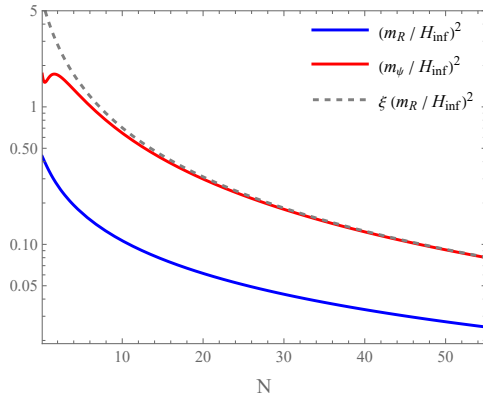


FIG. 2. Time-dependent mass-squared of the angular fluctuation ( $m_\psi^2$ ) and background radial mass-scale ( $m_R^2$ ) for B1.

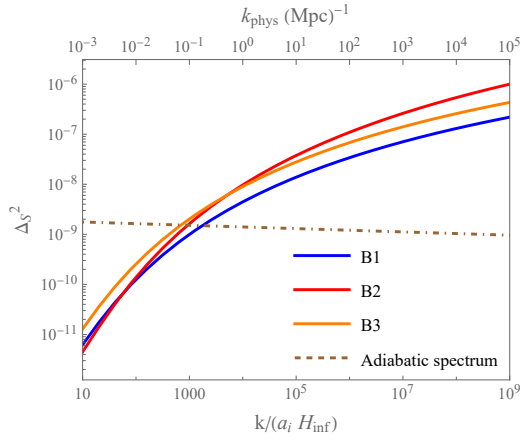


FIG. 3. Total matter isocurvature spectra for the benchmarks, assuming QCD axions constitute all DM via misalignment ( $r_a = 1$ ). We take  $H_{\infty} = 10^{13}$  GeV. Adiabatic spectrum also shown for  $A_s = 2.1 \times 10^{-9}$  and  $n_s = 0.967$  [12].

damping weakens for later-exiting modes. In the regime  $\delta = \xi(m_R/H_{\infty})^2 \lesssim 1$ , the dominant behavior is  $m_\psi^2 \simeq \xi m_R^2$ , i.e. the angular mode is enhanced relative to the flat case by the curvature lever arm  $\xi = R/L$ , while for  $\xi m_R^2 \gtrsim 1$  the negative curvature term  $\propto -\dot{R}^2$  reduces the effective axial mass.

Fig. 3 shows the resulting conserved superhorizon  $\Delta_S^2(k)$ . We take  $k/(a_i H_{\infty}) = 10$  to correspond to the CMB pivot scale  $k_* \simeq 0.002$  Mpc $^{-1}$ . Power is strongly suppressed on the largest CMB scales because those modes exit while  $m_\psi^2 \gtrsim H_{\infty}^2$ . As  $m_\psi^2/H_{\infty}^2$  decreases during the subsequent radial evolution, smaller scales are progressively less suppressed. The outcome is a blue-tilted isocurvature spectrum with running over the range of modes that probe the time variation of  $m_\psi^2$ , approaching a quasi-plateau once the angular mode becomes effectively light. Equivalently, the same scale-dependence can be understood kinematically from the conversion  $\delta\theta = \delta\psi/f(R)$ . For  $R \gg L$ ,  $f(R) = L \sinh(R/L)$  is exponentially sensitive to  $R$ , so slow-roll changes in  $R$

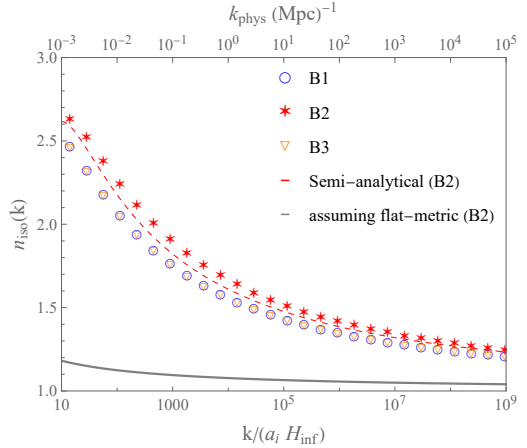


FIG. 4. Isocurvature spectral index  $n_{\text{iso}}(k)$  inferred from the numerical spectra. The red dashed curve shows the semi-analytic estimate in Eq. (24) for B2. The gray curve indicates the corresponding flat-metric expectation.

translate into strong,  $k$ -dependent suppression for modes exiting while  $R$  is evolving.

The benchmarks are chosen such that  $\Delta_S^2$  at CMB scales lies safely below current bounds, while smaller scales can be enhanced (with isocurvature-to-adiabatic ratio  $\sim \mathcal{O}(1)$  near  $k \sim 0.1$  Mpc $^{-1}$ , consistent with current limits [11, 12, 43]). This small-scale enhancement is a characteristic feature of the mechanism, and can be modulated by taking  $r_a < 1$ , varying  $(f_a, H_{\infty})$  within allowed bands, or modifying the radial trajectory (and thus  $m_\psi^2(t)$ ) through microscopic parameters.

A key result is that hyperbolic geometry can reopen parameter space that is excluded in the flat-metric case. In our benchmarks, we focus on  $H_{\infty} = 10^{13}$  GeV and  $f_a \sim 10^{14}\text{--}10^{16}$  GeV, since this lies near current upper limits and is therefore the most demanding regime for isocurvature. In contrast, for  $f(R) = R$  and comparable spectator trajectories, the angular mode remains effectively light, and satisfying the CMB bound at  $H_{\infty} = 10^{13}$  GeV typically requires  $R_i/f_a \sim 10^4\text{--}10^5$ , often implying super-Planckian displacements.

Fig. 4 shows the isocurvature tilt and its running inferred from numerical spectra shown in Fig. 3. When  $m_\psi^2/H_{\infty}^2$  varies slowly around horizon exit, the tilt is well approximated by the massive-mode estimate

$$n_{\text{iso}}(k) \simeq 4 - 2\sqrt{\frac{9}{4} - \frac{m_\psi^2(t(k))}{H_{\infty}^2}}, \quad (24)$$

with  $t(k)$  fixed by  $k = a(t)H_{\infty}$ . Evaluating  $m_\psi^2(t)$  using the numerical solution and substituting into Eq. (24) reproduces the approximate  $n_{\text{iso}}(k)$  as shown by the red dashed curve in Fig. 4 for B2.

In the slow-roll geometric domain, the hyperbolic metric ties the axial mass to the radial background through  $\xi \equiv R/L$ , implying a characteristic non-power-law running. For quartic PQ slow-roll, we give the following

scale-dependent mass template (see App. B)

$$m_\psi^2(k > k_m) \simeq m_\psi^2(k_m) \left[ 1 + \frac{2}{3} \left( \frac{m_\psi^2(k_m)}{H_{\text{inf}}^2 \xi_m} \right) \ln \left( \frac{k}{k_m} \right) \right]^{-3/2}, \quad (25)$$

where  $k_m$  is a matching scale at the onset of the geometric regime and  $\xi_m \equiv R_m/L$  controls the shape. A convenient prescription is to fix  $k_m$  by  $n_{\text{iso}}(k_m) = 2$ , equivalently  $m_\psi^2(k_m)/H_{\text{inf}}^2 = 5/4$ , so that for  $k \gtrsim k_m$  the entire running is governed by the single curvature parameter  $\xi_m$ , which labels the family of trajectories.

The salient point is the functional form. Combining the hyperbolic relation  $m_\psi^2 \propto \xi m_R^2 \propto R m_R^2$  with a quartic slow-roll trajectory yields

$$m_\psi^2(N) \propto (N - N_m)^{-3/2} \leftrightarrow m_\psi^2(k) \propto \left[ \ln \left( \frac{k}{k_m} \right) \right]^{-3/2}, \quad (26)$$

rather than the more familiar  $(N - N_m)^{-1}$  behavior typical of many slow-roll-induced runnings [44]. The extra half-power is the geometric fingerprint: it arises because the hyperbolic lever arm contributes an additional factor of  $R$  to the axial mass. Thus the scale-dependence is not well captured by a constant tilt or a simple broken power law, instead Eqs. (24) and (25) define a predictive template in which the running directly measures the field-space curvature through  $\xi_m$ . Fitting Fig. 4 gives  $\xi_m \simeq 12$  for B1, B3 and  $\xi_m \simeq 14.5$  for B2, which explains the apparent similarity of the isocurvature spectral shapes in Fig. 3.

## V. CONCLUSION

We have shown that the intrinsic geometry of the PQ field manifold can provide a minimal and symmetry-preserving solution to the standard axion isocurvature problem. For a hyperbolic PQ target-space metric, the angular fluctuation acquires a geometric, time-dependent effective mass during inflation, even in the absence of explicit PQ breaking in the axion potential. This dynamically suppresses CMB-scale isocurvature while generically yielding a new mechanism to generate blue-tilted spectrum. In benchmark realizations with  $H_{\text{inf}} = 10^{13} \text{ GeV}$ , the mechanism reopens parameter space at large  $f_a$  that is typically excluded in flat field-space.

Beyond enlarging the viable QCD-axion window for high-scale inflation, our results highlight a broader point: measurements of isocurvature scale-dependence can directly probe field-space curvature. We provided a compact phenomenological template that ties the running of the isocurvature tilt to a single curvature-controlled parameter, enabling model-agnostic tests of the mechanism and straightforward incorporation into future analyses. Several broad directions are motivated by this perspective. On the theory side, it will be important to develop controlled UV realizations of hyperbolic PQ metrics, and extend the framework to more general target spaces (non-constant curvature and/or non-diagonal

metrics). On the dynamics side, nontrivial background motion will be particularly interesting (such as  $\dot{\theta} \neq 0$  or post-inflationary evolution). Hyperbolic geometry can naturally support large angular velocities, making contact with rotating-field mechanisms such as Affleck-Dine dynamics in baryogenesis ([45]), axiogenesis [46] and kinetic-misalignment in [47], and more generally with additional signatures beyond the power spectrum [48, 49]. Finally, the generic enhancement of power on sub-CMB scales motivates systematic confrontation with small-scale probes, including Lyman- $\alpha$  forest [43], UV luminosity functions of high- $z$  galaxies [50], 21-cm measurements [51], and strong-lensing substructure [52], thereby enabling targeted searches for scale-dependent isocurvature as a window onto PQ field-space geometry.

## ACKNOWLEDGMENTS

We thank Peter Graham, Davide Racco, Raymond Co, and Tomo Takahashi for helpful comments and correspondence.

## Appendix A: An example of hyperbolic PQ field-space

In our setup the PQ sector is described by a single complex scalar  $\Phi$ , but we do not assume a flat field-space. At the level of a low-energy effective theory, the most general two-derivative kinetic term takes the form of a nonlinear sigma model,

$$\mathcal{L}_{\text{kin}} = \frac{1}{2} g_{ab}(\phi) \partial_\mu \phi^a \partial^\mu \phi^b, \quad (A1)$$

where  $\phi^a$  are the two real components of  $\Phi$ . The PQ symmetry is realized as a  $U(1)$  isometry of the target space (shifts of the angular coordinate), but the presence of this isometry does not fix the curvature. We now give a concrete example showing how a hyperbolic geometry can arise.

In  $\mathcal{N} = 1$  supergravity, scalar fields parameterize a Kähler manifold with metric ([53])

$$K_{i\bar{j}} = \frac{\partial^2 K}{\partial \phi^i \partial \bar{\phi}^j}, \quad (A2)$$

and kinetic term

$$\mathcal{L}_{\text{kin}} = K_{i\bar{j}} \partial_\mu \phi^i \partial^\mu \bar{\phi}^j. \quad (A3)$$

Appropriate choices of the Kähler potential  $K$  generate hyperbolic metrics already for a single complex field. A canonical example (familiar from  $\alpha$ -attractor models [54, 55]) is the “disk” Kähler potential

$$K(Z, \bar{Z}) = -3\alpha M_P^2 \ln \left( 1 - \frac{|Z|^2}{3M_P^2} \right), \quad (A4)$$

which yields the  $SU(1,1)/U(1)$ -invariant Kähler geometry.

For (A4) one finds

$$K_{Z\bar{Z}} = \frac{\alpha}{\left(1 - |Z|^2/(3M_P^2)\right)^2}. \quad (\text{A5})$$

Parametrizing the complex field as  $Z = \rho e^{i\theta}$ , the kinetic term is

$$\mathcal{L}_{\text{kin}} = \frac{\alpha}{\left(1 - \rho^2/(3M_P^2)\right)^2} \left[ (\partial\rho)^2 + \rho^2(\partial\theta)^2 \right]. \quad (\text{A6})$$

Matching to the sigma-model normalization  $\mathcal{L}_{\text{kin}} = \frac{1}{2} d\sigma^2$  gives  $g_{\rho\rho} = 2K_{Z\bar{Z}}$  and  $g_{\theta\theta} = 2K_{Z\bar{Z}}\rho^2$ . Defining the canonically normalized radial field  $R$  by

$$\frac{dR}{d\rho} = \sqrt{2K_{Z\bar{Z}}} = \frac{\sqrt{2\alpha}}{1 - \rho^2/(3M_P^2)}, \quad (\text{A7})$$

one obtains

$$R = \sqrt{6\alpha} M_P \tanh^{-1}\left(\frac{\rho}{\sqrt{3}M_P}\right). \quad (\text{A8})$$

Substituting back into (A6) yields the hyperbolic line element

$$d\sigma^2 = dR^2 + L^2 \sinh^2\left(\frac{R}{L}\right) d\theta^2, \quad L = \sqrt{\frac{3\alpha}{2}} M_P. \quad (\text{A9})$$

Note that  $R$  is unbounded,  $R \in [0, \infty)$ , so the regime  $R \gg L$  is readily accessible. The coordinate bound  $\rho < \sqrt{3}M_P$  corresponds to the disk boundary lying at infinite geodesic distance in field-space, i.e. it is a coordinate artifact rather than a physical restriction.

We do not assume a complete supersymmetric completion in our analysis; however, this example illustrates that a PQ-like complex scalar with hyperbolic field space arises naturally in  $\mathcal{N} = 1$  supergravity, with the target-space metric directly given by a well-motivated Kähler potential (and close cousins appearing widely in inflationary model building).

## Appendix B: Semi-analytic template for the tilt and its running

Here we sketch the derivation of the scale-space template used in the main text. We work in the slow-roll geometric regime  $\delta \equiv \xi(m_R/H)^2 \lesssim 1$  (where  $H \simeq H_{\text{inf}}$  is approximately constant) and take the potential to be quartic over the relevant field range.

*a. Geometric regime.* From Eq. (18) (or Eq. (17) in the  $R \gtrsim L$  limit), the dominant contribution to the canonically normalized angular mass is

$$m_\psi^2 \simeq \xi m_R^2, \quad \xi \equiv \frac{R}{L}, \quad m_R^2 \equiv \frac{V_{,R}}{R}, \quad (\text{B1})$$

where we neglect the subleading negative-curvature term  $\propto -\dot{R}^2$  in the slow-roll limit.

*b. Slow-roll background and  $N$ -scaling.* For quartic slow-roll,  $V_{,R} \simeq \lambda R^3$  and

$$3H\dot{R} \simeq -V_{,R} \simeq -\lambda R^3. \quad (\text{B2})$$

In terms of efolds  $N \equiv \ln a$  (so  $dN = Hdt$ ), this gives

$$\frac{dR}{dN} \simeq -\frac{\lambda}{3H^2} R^3 \quad \Rightarrow \quad \frac{1}{R^2(N)} = \frac{1}{R_m^2} + \frac{2\lambda}{3H^2} (N - N_m), \quad (\text{B3})$$

where  $N_m$  is a reference efold at which we match onto the geometric regime and  $R_m \equiv R(N_m)$ . Using  $m_R^2 = \lambda R^2$  and  $\xi = R/L$ , Eq. (B1) implies

$$m_\psi^2(N) \simeq \frac{\lambda}{L} R^3(N). \quad (\text{B4})$$

Combining with Eq. (B3) yields the characteristic falloff

$$m_\psi^2(N) \simeq m_{\psi,m}^2 \left[ 1 + \frac{2}{3} \left( \frac{m_{\psi,m}^2}{H^2 \xi_m} \right) (N - N_m) \right]^{-3/2}, \quad (\text{B5})$$

where  $m_{\psi,m}^2 \equiv m_\psi^2(N_m)$  and  $\xi_m \equiv R_m/L$ . (The identity used above is  $m_{\psi,m}^2/H^2 = \xi_m m_{R,m}^2/H^2$ .)

*c.  $k$ -space template.* For nearly constant  $H$ , horizon exit implies  $k = aH$  and hence

$$\ln\left(\frac{k}{k_m}\right) \simeq N - N_m, \quad (\text{B6})$$

with  $k_m \equiv a(N_m)H$ . Substituting Eq. (B6) into Eq. (B5) gives Eq. (25) in the main text,

$$m_\psi^2(k) \simeq m_\psi^2(k_m) \left[ 1 + \frac{2}{3} \left( \frac{m_\psi^2(k_m)}{H^2 \xi_m} \right) \ln\left(\frac{k}{k_m}\right) \right]^{-3/2}. \quad (\text{B7})$$

Together with the massive-mode estimate (24), this yields a unique analytic template for the tilt and its running for modes exiting after matching,  $k \gtrsim k_m$ .

*d. Choice of matching scale.* A convenient prescription is to define  $k_m$  by a fixed tilt value,

$$n_{\text{iso}}(k_m) = 2, \quad (\text{B8})$$

which using Eq. (24) is equivalent to  $m_\psi^2(k_m)/H^2 = 5/4$ . With this choice, the subsequent scale-dependence for  $k \gtrsim k_m$  is controlled by the single curvature parameter  $\xi_m$ .

In the geometric slow-roll regime one obtains for  $k \gtrsim k_m$ ,

$$m_\psi^2(N) \propto (N - N_m)^{-3/2} \leftrightarrow m_\psi^2(k) \propto \left[ \ln\left(\frac{k}{k_m}\right) \right]^{-3/2}, \quad (\text{B9})$$

which is the origin of the characteristic non-power-law running emphasized in the main text.

## Appendix C: Theoretical setup

We start from a canonically normalized complex scalar field  $\Phi$  with a  $U(1)$ -symmetric potential  $V(|\Phi|)$  and no explicit  $U(1)$ -breaking terms,

$$S = \int d^4x \sqrt{-g} \left[ -g^{\mu\nu} \partial_\mu \Phi^* \partial_\nu \Phi - V(|\Phi|) \right], \quad (\text{C1})$$

where  $g_{\mu\nu}$  is the spacetime metric and  $g \equiv \det g_{\mu\nu}$ . It is convenient to parameterize the complex field in polar coordinates,

$$\Phi(x) = \frac{R(x)}{\sqrt{2}} e^{i\theta(x)}, \quad (\text{C2})$$

so that  $|\Phi| = R/\sqrt{2}$  and the potential depends only on the radial field,  $V = V(R)$ .

In terms of  $(R, \theta)$ , the kinetic term becomes

$$-g^{\mu\nu} \partial_\mu \Phi^* \partial_\nu \Phi = -\frac{1}{2} g^{\mu\nu} (\partial_\mu R \partial_\nu R + R^2 \partial_\mu \theta \partial_\nu \theta), \quad (\text{C3})$$

and the action can be written in sigma-model form,

$$S = \int d^4x \sqrt{-g} \left[ -\frac{1}{2} G_{IJ}(\phi) g^{\mu\nu} \partial_\mu \phi^I \partial_\nu \phi^J - V(R) \right], \quad (\text{C4})$$

where  $\phi^I = (R, \theta)$  and the internal metric defines the field-space line element

$$\begin{aligned} d\sigma^2 &= G_{IJ}(\phi) d\phi^I d\phi^J \\ &= G_{RR} dR^2 + G_{\theta\theta} d\theta^2 + (G_{R\theta} + G_{\theta R}) dR d\theta. \end{aligned} \quad (\text{C5})$$

For the canonical complex scalar, the nonvanishing components are

$$G_{RR} = 1, \quad G_{\theta\theta} = R^2, \quad G_{R\theta} = G_{\theta R} = 0. \quad (\text{C6})$$

### 1. Nontrivial internal field-space metric

We now generalize to a complex scalar whose kinetic term defines a nontrivial (in general curved and non-Euclidean) field-space metric, while keeping a  $U(1)$ -symmetric potential  $V(R)$  with no explicit  $\theta$  dependence. As in Eq. (C5), we parameterize the internal line element as

$$d\sigma^2 = G_{IJ}(\phi) d\phi^I d\phi^J = dR^2 + f^2(R) d\theta^2, \quad (\text{C7})$$

where  $f(R)$  is an arbitrary function of the radial field. For simplicity we restrict to diagonal metrics ( $G_{R\theta} = G_{\theta R} = 0$ ). More general non-diagonal metrics can introduce kinetic mixing between  $R$  and  $\theta$  and lead to richer phenomenology. Absence of ghost instabilities requires a positive-definite metric, in particular  $f^2(R) > 0$ . The action becomes

$$\begin{aligned} S = \int d^4x \sqrt{-g} \left[ -\frac{1}{2} g^{\mu\nu} (\partial_\mu R \partial_\nu R + f^2(R) \partial_\mu \theta \partial_\nu \theta) \right. \\ \left. - V(R) \right], \end{aligned} \quad (\text{C8})$$

which reduces to the canonical flat-metric case when  $f(R) = R$ .

## 2. Background equations of motion

We consider homogeneous background fields,

$$R = R(t), \quad \theta = \theta(t), \quad (\text{C9})$$

on an FRW background with  $H \equiv \dot{a}/a$ . The reduced action is

$$S_{\text{bg}} = \int dt a^3(t) \left[ \frac{1}{2} \dot{R}^2 + \frac{1}{2} f^2(R) \dot{\theta}^2 - V(R) \right]. \quad (\text{C10})$$

The background equations can be written covariantly as

$$D_t \dot{\phi}^I + 3H \dot{\phi}^I + G^{IJ} V_{,J} = 0, \quad (\text{C11})$$

where  $\phi^I = (R, \theta)$ ,  $V_{,J} = \partial V / \partial \phi^J$ , and  $D_t$  is the covariant time derivative associated with  $G_{IJ}$ . For the metric (C7), the nonvanishing Christoffel symbols are

$$\Gamma_{\theta\theta}^R = -f(R) f'(R), \quad \Gamma_{R\theta}^\theta = \Gamma_{\theta R}^\theta = \frac{f'(R)}{f(R)}, \quad (\text{C12})$$

with  $f'(R) = df/dR$ . The  $R$  equation becomes

$$\ddot{R} + 3H\dot{R} - f(R) f'(R) \dot{\theta}^2 + V_{,R}(R) = 0, \quad (\text{C13})$$

and the  $\theta$  equation is

$$\ddot{\theta} + 2 \frac{f'(R)}{f(R)} \dot{R} \dot{\theta} + 3H\dot{\theta} = 0. \quad (\text{C14})$$

For a  $U(1)$ -symmetric potential, Eq. (C14) implies a conserved charge,

$$a^3(t) f^2(R) \dot{\theta} = \text{const.} \quad (\text{C15})$$

In this work we focus on the vanishing-charge sector,

$$\dot{\theta}_0 = 0, \quad \theta_0 = \text{const}, \quad (\text{C16})$$

for which the angular equation is automatically satisfied and the background evolution is purely radial,

$$\ddot{R}_0 + 3H\dot{R}_0 + V_{,R}(R_0) = 0. \quad (\text{C17})$$

Thus, in the zero-charge sector the homogeneous background does not depend explicitly on the choice of  $f(R)$ .

## 3. Fluctuations: radial $\delta R$ and canonical axial $\delta\psi$

We now consider linear fluctuations about the homogeneous background,

$$R(t, \mathbf{x}) = R_0(t) + \delta R(t, \mathbf{x}), \quad \theta(t, \mathbf{x}) = \theta_0 + \delta\theta(t, \mathbf{x}), \quad (\text{C18})$$

and work in a fixed FRW/de Sitter background (spatially flat gauge), neglecting metric perturbations. Expanding Eq. (C8) to quadratic order, one finds that  $\delta R$  and  $\delta\theta$  decouple at linear order when  $\dot{\theta}_0 = 0$ , with quadratic action

$$S^{(2)} = \int d^4x a^3(t) \left[ \frac{1}{2} \left( \dot{\delta R}^2 - \frac{(\nabla \delta R)^2}{a^2} - V_{,RR}(R_0) \delta R^2 \right) + \frac{1}{2} f^2(R_0) \left( \dot{\delta\theta}^2 - \frac{(\nabla \delta\theta)^2}{a^2} \right) \right], \quad (\text{C19})$$

where derivatives of  $V$  are evaluated on  $R_0(t)$ . Varying with respect to  $\delta R$  gives

$$\ddot{\delta R} + 3H\dot{\delta R} - \frac{\nabla^2}{a^2} \delta R + V_{,RR}(R_0) \delta R = 0. \quad (\text{C20})$$

The angular fluctuation is not canonically normalized. Defining the canonical axial fluctuation

$$\delta\psi(t, \mathbf{x}) \equiv f(R_0(t)) \delta\theta(t, \mathbf{x}), \quad (\text{C21})$$

the  $\delta\theta$  equation can be rewritten in Klein–Gordon form,

$$\ddot{\delta\psi} + 3H\dot{\delta\psi} - \frac{\nabla^2}{a^2} \delta\psi + m_\psi^2(t) \delta\psi = 0, \quad (\text{C22})$$

with time-dependent effective mass

$$m_\psi^2(t) = \frac{f'(R_0)}{f(R_0)} V_{,R}(R_0) - \frac{f''(R_0)}{f(R_0)} \dot{R}_0^2. \quad (\text{C23})$$

Thus, in the vanishing-charge background, the internal geometry affects the linear dynamics through the axial perturbations, while the radial perturbation  $\delta R$  is governed by the usual potential curvature  $V_{,RR}(R_0)$ .

---

[1] R. D. Peccei and H. R. Quinn, CP Conservation in the Presence of Instantons, *Phys. Rev. Lett.* **38**, 1440 (1977).

[2] R. D. Peccei and H. R. Quinn, Constraints Imposed by CP Conservation in the Presence of Instantons, *Phys. Rev. D* **16**, 1791 (1977).

[3] S. Weinberg, A New Light Boson?, *Phys. Rev. Lett.* **40**, 223 (1978).

[4] F. Wilczek, Problem of Strong  $P$  and  $T$  Invariance in the Presence of Instantons, *Phys. Rev. Lett.* **40**, 279 (1978).

[5] D. J. E. Marsh, Axion Cosmology, *Phys. Rept.* **643**, 1 (2016), arXiv:1510.07633 [astro-ph.CO].

[6] L. Di Luzio, M. Giannotti, E. Nardi, and L. Visinelli, The landscape of QCD axion models, *Phys. Rept.* **870**, 1 (2020), arXiv:2003.01100 [hep-ph].

[7] J. Preskill, M. B. Wise, and F. Wilczek, Cosmology of the Invisible Axion, *Phys. Lett. B* **120**, 127 (1983).

[8] L. F. Abbott and P. Sikivie, A Cosmological Bound on the Invisible Axion, *Phys. Lett. B* **120**, 133 (1983).

[9] M. Dine and W. Fischler, The Not So Harmless Axion, *Phys. Lett. B* **120**, 137 (1983).

[10] M. Badziak and K. Harigaya, Naturally astrophobic QCD axion, *JHEP* **06**, 014, arXiv:2301.09647 [hep-ph].

[11] D. J. H. Chung and A. Upadhye, Search for strongly blue axion isocurvature, *Phys. Rev. D* **98**, 023525 (2018), arXiv:1711.06736 [astro-ph.CO].

[12] Y. Akrami *et al.* (Planck), Planck 2018 results. X. Constraints on inflation, *Astron. Astrophys.* **641**, A10 (2020), arXiv:1807.06211 [astro-ph.CO].

[13] E. Calabrese *et al.* (Atacama Cosmology Telescope), The Atacama Cosmology Telescope: DR6 constraints on extended cosmological models, *JCAP* **11**, 063, arXiv:2503.14454 [astro-ph.CO].

[14] M. P. Hertzberg, M. Tegmark, and F. Wilczek, Axion Cosmology and the Energy Scale of Inflation, *Phys. Rev. D* **78**, 083507 (2008), arXiv:0807.1726 [astro-ph].

[15] T. Higaki, K. S. Jeong, and F. Takahashi, Solving the Tension between High-Scale Inflation and Axion Isocurvature Perturbations, *Phys. Lett. B* **734**, 21 (2014), arXiv:1403.4186 [hep-ph].

[16] K. Choi, E. J. Chun, S. H. Im, and K. S. Jeong, Diluting the inflationary axion fluctuation by a stronger QCD in the early Universe, *Phys. Lett. B* **750**, 26 (2015), arXiv:1505.00306 [hep-ph].

[17] R. T. Co, E. Gonzalez, and K. Harigaya, Axion Misalignment Driven to the Bottom, *JHEP* **05**, 162, arXiv:1812.11186 [hep-ph].

[18] L. Heurtier, F. Huang, and T. M. P. Tait, Resurrecting low-mass axion dark matter via a dynamical QCD scale, *JHEP* **12**, 216, arXiv:2104.13390 [hep-ph].

[19] M. Berbig, Minimal solution to the axion isocurvature problem from nonminimal coupling, *Phys. Rev. D* **110**, 095008 (2024), arXiv:2404.06441 [hep-ph].

[20] P. Chakraborty, J. Cheng, M. Reece, and Z. Wang, A Step in Flux to Suppress Axion Isocurvature, (2025), arXiv:2507.12519 [hep-ph].

[21] J. Kearney, N. Orlofsky, and A. Pierce, High-Scale Axions without Isocurvature from Inflationary Dynamics, *Phys. Rev. D* **93**, 095026 (2016), arXiv:1601.03049 [hep-ph].

[22] M. Kamionkowski and J. March-Russell, Planck scale physics and the Peccei–Quinn mechanism, *Phys. Lett. B* **282**, 137 (1992), arXiv:hep-th/9202003.

[23] S. M. Barr and D. Seckel, Planck scale corrections to axion models, *Phys. Rev. D* **46**, 539 (1992).

[24] S. Kasuya, M. Kawasaki, and T. Yanagida, Cosmological axion problem in chaotic inflationary universe, *Phys. Lett. B* **409**, 94 (1997), arXiv:hep-ph/9608405.

[25] S. Kasuya, M. Kawasaki, and T. Yanagida, Domain wall problem of axion and isocurvature fluctuations in chaotic inflation models, *Phys. Lett. B* **415**, 117 (1997), arXiv:hep-ph/9709202.

- [26] M. Kawasaki, T. T. Yanagida, and K. Yoshino, Domain wall and isocurvature perturbation problems in axion models, *JCAP* **11**, 030, arXiv:1305.5338 [hep-ph].
- [27] E. J. Chun, Axion Dark Matter with High-Scale Inflation, *Phys. Lett. B* **735**, 164 (2014), arXiv:1404.4284 [hep-ph].
- [28] K. Nakayama and M. Takimoto, Higgs inflation and suppression of axion isocurvature perturbation, *Phys. Lett. B* **748**, 108 (2015), arXiv:1505.02119 [hep-ph].
- [29] K. Harigaya, M. Ibe, M. Kawasaki, and T. T. Yanagida, Dynamics of Peccei-Quinn Breaking Field after Inflation and Axion Isocurvature Perturbations, *JCAP* **11**, 003, arXiv:1507.00119 [hep-ph].
- [30] T. Kobayashi and F. Takahashi, Cosmological Perturbations of Axion with a Dynamical Decay Constant, *JCAP* **08**, 056, arXiv:1607.04294 [hep-ph].
- [31] I. J. Allali, M. P. Hertzberg, and Y. Lyu, Altered axion abundance from a dynamical Peccei-Quinn scale, *Phys. Rev. D* **105**, 123517 (2022), arXiv:2203.15817 [hep-ph].
- [32] M. Fairbairn, R. Hogan, and D. J. E. Marsh, Unifying inflation and dark matter with the Peccei-Quinn field: observable axions and observable tensors, *Phys. Rev. D* **91**, 023509 (2015), arXiv:1410.1752 [hep-ph].
- [33] P. W. Graham and D. Racco, Revisiting isocurvature bounds on the minimal QCD axion, *JHEP* **12**, 028, arXiv:2506.03348 [hep-ph].
- [34] S. Kasuya and M. Kawasaki, Axion isocurvature fluctuations with extremely blue spectrum, *Phys. Rev. D* **80**, 023516 (2009), arXiv:0904.3800 [astro-ph.CO].
- [35] D. J. H. Chung and H. Yoo, Elementary Theorems Regarding Blue Isocurvature Perturbations, *Phys. Rev. D* **91**, 083530 (2015), arXiv:1501.05618 [astro-ph.CO].
- [36] D. J. H. Chung and S. C. Tadepalli, Large blue spectral index from a conformal limit of a rotating complex scalar, *Phys. Rev. D* **111**, 083527 (2025), arXiv:2406.12976 [astro-ph.CO].
- [37] A. R. Brown, Hyperbolic Inflation, *Phys. Rev. Lett.* **121**, 251601 (2018), arXiv:1705.03023 [hep-th].
- [38] S. Mizuno and S. Mukohyama, Primordial perturbations from inflation with a hyperbolic field-space, *Phys. Rev. D* **96**, 103533 (2017), arXiv:1707.05125 [hep-th].
- [39] C.-B. Chen and J. Soda, Geometric structure of multi-form-field isotropic inflation and primordial fluctuations, *JCAP* **05** (05), 029, arXiv:2201.03160 [hep-th].
- [40] L. Iacconi and D. J. Mulryne, Multi-field inflation with large scalar fluctuations: non-Gaussianity and perturbativity, *JCAP* **09**, 033, arXiv:2304.14260 [astro-ph.CO].
- [41] M. De Angelis and C. van de Bruck, Adiabatic and isocurvature perturbations in extended theories with kinetic couplings, *JCAP* **10**, 023, arXiv:2304.12364 [hep-th].
- [42] G. Grilli di Cortona, E. Hardy, J. Pardo Vega, and G. Villadoro, The QCD axion, precisely, *JHEP* **01**, 034, arXiv:1511.02867 [hep-ph].
- [43] M. R. Buckley, P. Du, N. Fernandez, and M. J. Weichert, General constraints on isocurvature from the CMB and Ly- $\alpha$  forest, *JCAP* **12**, 006, arXiv:2502.20434 [astro-ph.CO].
- [44] D. H. Lyth and A. Riotto, Particle physics models of inflation and the cosmological density perturbation, *Phys. Rept.* **314**, 1 (1999), arXiv:hep-ph/9807278.
- [45] I. Affleck and M. Dine, A new mechanism for baryogenesis, *Nuclear Physics B* **249**, 361 (1985).
- [46] R. T. Co and K. Harigaya, Axiogenesis, *Phys. Rev. Lett.* **124**, 111602 (2020), arXiv:1910.02080 [hep-ph].
- [47] R. T. Co, L. J. Hall, and K. Harigaya, Axion Kinetic Misalignment Mechanism, *Phys. Rev. Lett.* **124**, 251802 (2020), arXiv:1910.14152 [hep-ph].
- [48] S. Renaux-Petel, Inflation with strongly non-geodesic motion: theoretical motivations and observational imprints, *PoS* **EPS-HEP2021**, 128 (2022), arXiv:2111.00989 [astro-ph.CO].
- [49] H. Firouzjahi, M. A. Gorji, S. Mukohyama, and A. Talebian, Dark matter from entropy perturbations in curved field space, *Phys. Rev. D* **105**, 043501 (2022), arXiv:2110.09538 [gr-qc].
- [50] S. Yoshiura, M. Oguri, K. Takahashi, and T. Takahashi, Constraints on primordial power spectrum from galaxy luminosity functions, *Phys. Rev. D* **102**, 083515 (2020), arXiv:2007.14695 [astro-ph.CO].
- [51] T. Minoda, S. Yoshiura, and T. Takahashi, Probing isocurvature perturbations with 21-cm global signal in the light of HERA result, *Phys. Rev. D* **105**, 083523 (2022), arXiv:2112.15135 [astro-ph.CO].
- [52] N. Dalal and C. S. Kochanek, Strong lensing constraints on small scale linear power, (2002), arXiv:astro-ph/0202290.
- [53] J. Wess and J. Bagger, *Supersymmetry and supergravity* (Princeton University Press, Princeton, NJ, USA, 1992).
- [54] J. J. M. Carrasco, R. Kallosh, and A. Linde, Cosmological Attractors and Initial Conditions for Inflation, *Phys. Rev. D* **92**, 063519 (2015), arXiv:1506.00936 [hep-th].
- [55] J. J. M. Carrasco, R. Kallosh, A. Linde, and D. Roest, Hyperbolic geometry of cosmological attractors, *Phys. Rev. D* **92**, 041301 (2015), arXiv:1504.05557 [hep-th].